Cyclic Ketones as Future Fuels: Reactivity with OH Radicals

Dapeng Liu, Binod Raj Giri*, Aamir Farooq*

King Abdullah University of Science and Technology, Clean Combustion Research Center,

Physical Sciences and Engineering Division, Thuwal 23955-6900, Saudi Arabia

*Corresponding Author: binod.giri@kaust.edu.sa
aamir.farooq@kaust.edu.sa

Abstract

For a sustainable energy future, research directions should orient towards exploring new fuels suitable for future advanced combustion engines to achieve better engine efficiency and significantly less harmful emissions. Cyclic ketones, among bio-derived fuels, are of significant interest to the combustion community for several reasons. As they possess high resistance to auto-ignition characteristics, they can potentially be attractive for fuel blending applications to increase engine efficiency and also to mitigate harmful emissions. Despite their importance, very few studies are rendered in understanding of the chemical kinetic behavior of cyclic ketones under engine-relevant conditions. In this work, we have conducted an experimental investigation for the reaction kinetics of OH radicals with cyclopentanone (CPO) and cyclohexaneone (CHO) for the first time over a wide range of experimental conditions (T = 900 – 1330 K, and p ~ 1.2 bar) in a shock tube. Reaction kinetics was followed by monitoring UV laser absorption of OH radicals near 306.7 nm. Our measured rate coefficients, with an overall uncertainty (2σ) of ± 20%, can be expressed in Arrhenius form as (in units of $cm^3molecule^{-1}s^{-1}$):

$$k_1(\mathrm{CPO + OH}) = 1.20 \times 10^{-10} \exp\left(-2115\,\frac{K}{T}\right) \qquad (902 – 1297\ \mathrm{K})$$

$$k_2(\mathrm{CHO + OH}) = 2.11 \times 10^{-10} \exp\left(-2268\,\frac{K}{T}\right) \qquad (935 – 1331\ \mathrm{K})$$

Combining our measured data with the single low-temperature literature data, the following three-parameter Arrhenius expressions (in units of $cm^3molecule^{-1}s^{-1}$) are obtained over a wider temperature range:

$$k_1(\mathrm{CPO + OH}) = 1.07 \times 10^{-13} \left(\frac{T}{300\ K}\right)^{3.20} \exp\left(1005.7\,\frac{K}{T}\right) \qquad (298 – 1297\ \mathrm{K})$$

$$k_2(\mathrm{CHO + OH}) = 3.12 \times 10^{-13} \left(\frac{T}{300\ K}\right)^{2.78} \exp\left(897.5\,\frac{K}{T}\right) \qquad (298 – 1331\ \mathrm{K})$$

Discrepancies between the theoretical and current experimental results are observed. Earlier theoretical works are found to over-predict our measured rate coefficients. Interestingly, these cyclic ketones exhibit similar reactivity behavior as that of their linear ketone counterparts over the experimental conditions of this work.

1. Introduction

As the global energy portfolio stands today, it appears that petroleum-based fuels will remain primary source of energy to power industry and transportation sectors for some decades to come. The renewable sources of energy are foreseen to increase their share up to 10% by 2040. Global demand for petroleum-based fuels is rising at ~1% annual rate to power internal combustion engines (ICE) in the transport sector.[1] This is progressively adding up the challenges for curbing environmental pollution and greenhouse gas emission. The growing concerns over global warming and diminishing petroleum reserves have led scientists and engineers to focus on improving combustion technology, e.g., by developing new fuel-engine systems.

Recently, there is a growing interest on engine-fuel design optimization due to stringent emission regulations worldwide.[2-6] At present, the trends in the development of more efficient modern spark ignition (SI) engines are moving towards increasing the compression ratio and implementing turbocharging.[4] The drawback of doing so is that it may cause engine knocking, or even super-knock, as the ignition delay times (IDTs) of fuel-air mixtures drop sharply with increasing cylinder intake pressure. Therefore, fuels having high anti-knock quality are quite attractive to mitigate engine knocking events in modern SI engines. To this end, cyclic ketones are of significant interest to the combustion community because these fuels are found to have positive impacts on enhanced engine performance and low pollutant emissions. Recently, Co-Optima researchers evaluated 41 blendstocks from various chemical families, e.g., hydrocarbons (alkanes, alkenes and aromatics) and oxygenates (alcohols, esters, ethers, ketones), in the Tier 2 survey to assess their potential of increasing the efficiency of future advanced SI engines.[7-8] The blendstock survey "Tier 2" identified eight fuel blendstocks, one

being cyclopentanone, meeting the merit function criteria for the detailed blendstock evaluation "Tier 3" to realize their introduction in the market by 2025-2035.

Cyclic ketones appear very promising among the various renewable bio-derived fuels. Cyclic ketones can be effectively produced *via* chemical and biochemical conversion technology, e.g., breaking down of lignocellulosic biomass by endophytic fungi, pyrolysis of biomass or hydrogenation of biomass derived furfural[9-12]. These ketones display interesting and desirable combustion characteristics as the potential candidates for alternatives to petroleum-based fuels for various reasons, such as: i) they possess high resistance to auto-ignition (RON ~ 100)[13], making it favorable for application in spark-ignition internal combustion engines[14]; ii) they are very effective in reducing the harmful emissions of greenhouse gases, particulate matter and soot[15,16]. For instance, a recent experimental study in direct injection diesel engine by Boot et al.[15] found cyclohexanone performing exceptionally well for soot abatement as compared to other oxygenates such as tripropylene glycol, methyl ether and dibutyl maleate. Ethers are known to be most effective in reducing soot emission among oxygenates (see Boot el. al [15] and references cited therein.); iii) they are found to be promising chemical feedstock for the synthesis of high-density fuels like polycylic alkanes which can be blended into conventional aviation fuels for increased volumetric heating values.[17-18] Ketones also appear as important intermediates during the low-temperature combustion of large hydrocarbons and oxygenated fuels. Despite their importance in combustion, only few studies have been dedicated to understand the combustion behavior of cyclic ketones.[15-16, 19-26]

Giri et al.[23] recently reported experimental and theoretical rate coefficients for the thermal unimolecular decomposition of cyclopentanone (CPO). Their master equation results were consistent with the experimental results, indicating that CPO almost exclusively (> 95%) decomposes to produce CO and C_2H_4. Thion et al.[20] studied the oxidation kinetics of CPO in a jet-stirred reactor over a wide range of experimental conditions (T = 730 – 1280 K, p = 1 and

10 atm, and equivalence ratio (φ) = 0.5, 1 and 2). Additionally, they performed *ab initio*/RRKM-master equation calculations to predict rate coefficients for H-abstraction reactions of CPO by important combustion species (H, OH and CH_3) and constructed an extended chemical kinetic model to validate experimentally measured reaction intermediates and products. Through reaction flux analyses, they found that hydrogen abstraction from the β-carbon site (see R1 in Fig. 1), resulting into β-cyclopentanonyl (β-CPOnyl) radical accounts major percentage of CPO consumption; whereas the formation of α-cyclopentanonyl (α-CPOnyl) radical makes a minor contribution accounting for only 28% consumption under stoichiometric conditions at 850 K, 10 atm. The incipient radicals have major effect in the overall oxidation kinetics of CPO because α-CPOnyl is resonantly stabilized radical and is thus less reactive than β-CPOnyl radical. Therefore, the branching ratio of hydrogen abstraction reaction of CPO is of high importance for combustion modeling. Thion et al.[20] further observed that OH-initiated oxidation of CPO dominates between 850 and 1050 K, and H-abstraction by H atoms take the lead beyond 1050 K. Finally, they realized a room for improvement of the kinetic model and demanded for additional measurements such as ignition delay times (IDTs) and laminar burning velocities to better understand the chemistry of CPO. Very recently, Zhang et al.[19] investigated CPO oxidation by using a high-pressure shock tube and a rapid compression machine over a wide range of experimental condition (T = 794 – 1368 K, p = 15 and 30 bar, φ = 0.5, 1.0 and 2.0). They measured ignition delay times (IDTs) and CO time-histories during CPO oxidation and also performed *ab initio*/transition state theory calculations to derive the high-pressure limiting rate coefficients for the unimolecular decomposition of cyclopentanonyl peroxy radicals ($C_5H_7O_3$) forming cyclopentenone (C_5H_6O) and HO_2. By incorporating the newly derived rate coefficients for $C_5H_7O_3$ radicals, they developed a detailed kinetic model comprising of 444 species and 2269 reactions to describe the combustion behavior of CPO in their experiments. Overall, the kinetic model performed satisfactorily to reproduce their

experimental data except that of the simulated IDTs at 1 atm which over-predicted experimentally measured IDTs. The authors noted the importance of the branching ratio of α- and β-CPOnyl radicals in the overall oxidation kinetics of CPO. Similar to Thion et al.[20], they arrived to a similar conclusion that the formation of β-CPOnyl radicals takes the major reaction flux during CPO oxidation. Their results showing the dominance of the β-CPOnyl radicals is probably not surprising considering the fact that the rate coefficients for reaction (R1), $k_1 = k_{1\alpha} + k_{1\beta}$, and the subsequent decomposition of the α- and β -CPOnyl radicals were adopted from Zhou et al.[21]. Zhou et al.[21] used *ab initio*/RRKM-ME calculations to show that reaction R1 predominantly occurs at the β-site with slightly decreasing importance at higher temperatures, e.g., $k_{1\beta}/ k_{1\alpha}$ is 1.89 and 1.5 at 500 K and 1400 K, respectively. Their predicted value of rate coefficient is faster by a factor of two than that of a single room-temperature measurement from Dagaut et al. [27] who derived k_1 (298 K) = (2.94 ± 0.18) × 10^{-12} cm^3 $molecule^{-1}$ s^{-1} using flash photolysis / resonance fluorescence technique. Theoretical rate coefficient of Thion et al.[20] also over-predicts the experimental value by ~30%. The predictions of overall rate coefficients of R1 and the branching ratios from the two theoretical studies[20-21] do not show good agreement. Both studies exhibit different temperature dependence of the rate coefficients. Therefore, there is a need to provide accurate rate coefficients for the hydrogen abstraction reaction to build a robust combustion model.

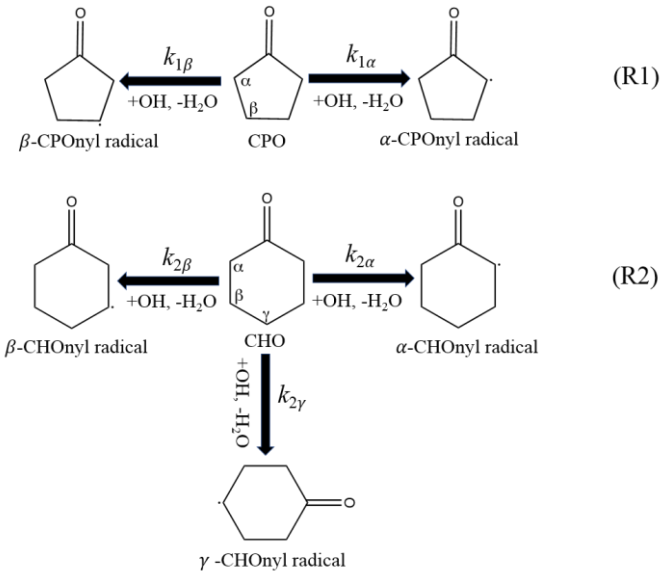

Figure 1: Hydrogen abstraction pathways for the reaction of cyclopentanone (CPO) and cyclohexanone (CHO) with OH radicals.

As for cyclohexanone (CHO), a recent paper by He et al.[26] provides a brief literature review. Serinyel et al.[25] studied the kinetics of CHO oxidation in a jet stirred reactor (JSR) over a wide range of experimental conditions (T = 530 – 1220 K, p = 10 atm and φ = 0.5 – 4). They measured various species (reactants, intermediates and products) using gas chromatography and FTIR spectroscopy. They proposed a detailed kinetic model to reasonably describe their experimental results of CHO oxidation. However, their kinetic model did not accurately predict experimentally measured concentrations of all species. For this reason, the authors demanded for more experimental data to fully validate the proposed mechanism. Aiming for a better combustion model of cyclohexanone, He et al.[26] measured ignition delay times of cyclohexanone behind reflected shock waves over p = 2.5 – 10 atm, T = 1255 - 1646 K and φ = 0.5 – 2.0. The authors compared their measured values with the predictions from earlier kinetic model[25] and found that the model over-predicted their measurements by 30 – 50%. This motivated them to modify the earlier kinetic model[25] by identifying key chemical reactions and updating their rate coefficients. Their modified kinetic model performed satisfactorily to reproduce their experimental data and previous JSR data. Moreover, the authors noted that

hydrogen abstraction reactions of CHO play significant role, and the partitioning of α, β and γ -CHOnyl radicals (see R2 in Fig. 1) shows different sensitivity towards CHO oxidation. For example, H-abstraction from the α-site of CHO, resulting in α-CHOnyl radical, was found to increase the global reactivity, whereas the formation of β-CHOnyl has the opposite effect. Contrary to the CPO oxidation model, the modified kinetic model from He et al.[26] predicted the H-abstraction reaction at the α-site of CHO to be the dominant channel. Thion et al.[28] recently also proposed an improved kinetic model for CHO oxidation by validating against their new JSR measurements to complement their earlier work.[25] Their improved model favored the formation of β-CHOnyl radical as opposed to α-CHOnyl contradicting the earlier models. However, this is in line with the kinetic model of CPO oxidation. They further performed G3//MP2/aug-cc-pVDZ and RRKM-ME calculations to obtain rate coefficients for important reactions, e.g., H-abstraction reaction from CHO by H, OH and CH_3 radicals, isomerization and decomposition of α, β, γ -CHOnyl radicals. Based on their new JSR experimental and computational results, they updated Serinyel et al.'s model[25] and validated against the available data. However, we note here that the newly derived theoretical rate coefficients from this study are not validated against the experimentally measured kinetic data. The only available room-temperature experimental value reported by Dagaut et al. [27] k_2 (298 K) = (6.39 ± 0.51) × 10^{-12} cm^3 s^{-1} is faster by 45% than that of theory.[28] Therefore, there is a need for an experimental study of the rate coefficients of CHO + OH reaction under combustion relevant conditions.

There are several motivations for the current work: i) from future fuels prospective, cyclic ketones are of significant interest to the combustion community; ii) the oxidation of cyclic ketones by OH radicals is one of the most important initiation step, and no direct measurements of rate coefficients of reaction R1 ($k_1 = k_{1\alpha} + k_{1\beta}$) and reaction R2 ($k_2 = k_{2\alpha} + k_{2\beta} + k_{2\gamma}$) are yet available at high temperatures; iii) As explained above, the oxidation kinetics of cyclic ketones is sensitive to the branching ratio of R1 and R2 which led to the disparity in

terms of the performance of the available kinetic models; iii) large discrepancies exist among the theoretical predictions of the rate coefficients. Through this work, we aim to resolve the discrepancies in the literature by providing reliable data for the rate coefficient of R1 and R2 over a broad range of experimental conditions. To our knowledge, this is the first experimental investigation for the rate coefficients of CPO + OH (R1) and CHO + OH (R2) at high temperatures.

2. Experimental Method

The reaction kinetics of OH radicals with C_5-C_6 cyclic ketones was investigated over the temperature range of 900 K and 1300 K, and pressures near 1.2 bar using a low-pressure shock tube (LPST) and UV laser diagnostic facility at KAUST. The experimental facility and diagnostic method have been detailed previously.[29-30] The stainless steel shock tube has a 9 m long driven section and a variable length driver section, and both sections have an internal diameter of 14.2 cm. In this study, a 3 m long driver section was used to achieve a test time of ~1.5 ms behind reflected shock waves. The shock waves were generated by pressure bursting of polycarbonate diaphragms of 5 mm thickness and using helium as driver gas. The desired temperature and pressure behind reflected shock waves were achieved by tailoring the pressure differential across the diaphragm. A series of five piezoelectric transducers (PCB 113B26) over the last 1.5 m of the driven section were employed to measure the incident shock speed. The temperature and pressure behind reflected shock waves were calculated by using measured incident shock speed and thermodynamic data of the test gas mixture and by employing shock-jump relations [31] embedded in the Frosh code [32].

Hydroxyl radicals were generated *via* fast thermal decomposition of a well-known clean OH precursor, *tert*-butyl hydroperoxide (TBHP)[33]. The reaction kinetics of the title reaction was followed by monitoring OH radical decay near 307 nm *via* a narrow linewidth cw laser

system comprised of an Nd:YAG 532 nm pump laser, a ring-dye visible laser and a frequency doubler. The UV light was tuned precisely to the center (306.6868 nm) of the well-characterized R1(5) absorption line in the (0, 0) vibrational band of the $A^2\,\Sigma^+ \leftarrow X^2\,\Pi$ electronic system of OH radical. For optical detection of OH radicals, the laser beam was guided through the cross-section of the shock tube *via* two quartz windows which are installed 2 cm away from the shock tube end wall. Two modified Thorlab PDA36-EC photodetectors (spectral range 305 -1100 nm) served to measure the laser intensity before and after the shock tube. The noise of the laser beam after common-mode-rejection was less than 0.1% of the signal. The laser intensity time-profile was quantitatively converted into OH mole fraction (X_{OH}) time-profile by using Beer-Lambert law.

The purity of used chemicals was: 99% CHO and CPO (Sigma Aldrich; further purified through freeze-pump-thaw cycle), 70% TBHP solution in water (Sigma Aldrich), helium (99.9%) and argon (99.999%) from Abdullah Hashim Gases. The desired gas mixtures were prepared manometrically in a 24 litre Teflon-coated stainless-steel vessel equipped with a magnetically driven stirrer. The mixtures were left for at least two hours to ensure homogeneity. Prior to mixture preparation, the mixing vessel was turbo-pumped down to 10^{-5} mbar. Partial pressures of cyclic ketones and TBHP were measured accurately using a 0-20 Torr MKS Baratron pressure gauge. For all measurements, an excess concentration of cyclic ketone (at least 10 times) as compared to that of OH radicals was used to ensure that OH radical decay will follow first-order kinetics.

3. Results and Discussion

Measurements were carried out behind reflected shock waves at ~ 1.2 bar and varying temperatures between 900 – 1300 K; experimental conditions are listed in Table 1. Two test

gas mixtures of varying CPO and CHO concentrations were employed to ensure that the reaction under investigation is obeying pseudo first-order kinetics. Figure 2 illustrates a representative OH time-history measured at 1218 K and 1.13 bar for CPO + OH (R1); the inset in Fig. 2 displays ln[OH] vs time plot demonstrating that OH decay follows first-order kinetics. In such cases, the rate coefficients can be directly calculated from the pseudo first order plot. However, this methodology of extracting the rate coefficients can't be applied at lower temperatures (<950 K). Below 950 K, the decomposition of TBHP is slow, and the OH rise time becomes of the order of the decay time - (see CPO + OH data measured at 902 K and 1.26 bar presented in the Supporting Information as an example). Therefore, detailed kinetic model is critically important to accurately determine the rate coefficients for reactions R1 and R2 to account for the effect of OH build up kinetics and OH loss by unwanted reactions e.g. CH_3 + OH. For the detailed model, we added TBHP sub-mechanism of Pang et al.[34] to the existing kinetic models for CPO and CHO developed by Thion et al.[20] and Serinyel et al.[25], respectively. We iteratively varied the rate coefficient of the target reaction to obtain the best match between the experimental and simulated OH profiles. We employed Chemkin-Pro[35] software to simulate OH profiles using zero-dimensional batch reactor and constant *U*,*V* constraints. The red line in Fig. 2 demonstrates an example of such simulation result, and also shown is the perturbation of ± 50% from the best-fit value (k_1 = 2.39 × 10^{-11} $cm^3molecule^{-1}s^{-1}$ at 1218 K, 1.13 bar) − more examples are provided in the Supporting Information. The perturbation analysis shows strong sensitivity of k_1 towards OH decay. Further hydroxyl radical sensitivity analyses show negligible contribution from secondary chemistries on the measured OH time-history (see Fig. 3). Also, we found negligible influence of the branching ratio on our determined overall rate coefficients. Accounting for uncertainties in the temperature (± 0.7%) of reflected shock wave, fitting the measured OH profile (± 6%), OH absorption coefficient (± 3%), test gas composition

(± 5%), and locating time zero (± 0.5 μs) gives an overall uncertainty (2σ) of ± 20% in our measured values of the rate coefficients.

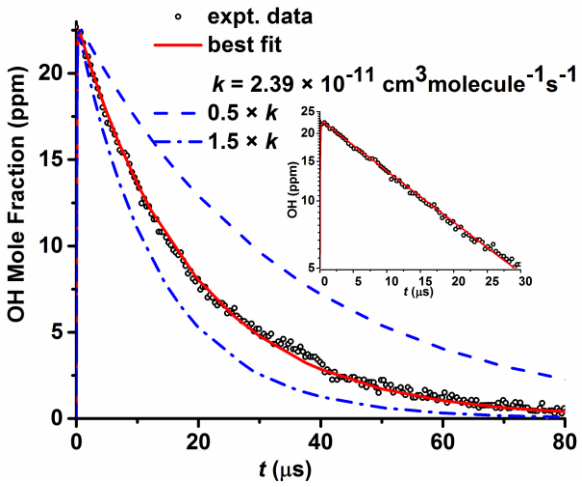

Figure 2. A representative OH time-history plot for CPO + OH → products (R1) at 1218 K and 1.13 bar. Mixture composition: 300 ppm CPO and 22 ppm TBHP (~ 51 ppm H_2O) in argon.

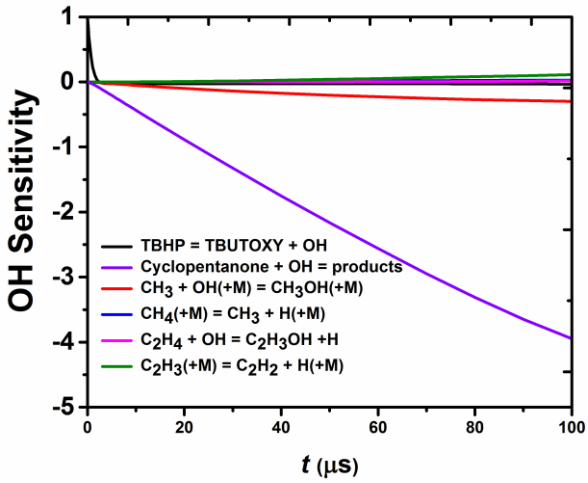

Figure 3. Hydroxyl radical sensitivity analysis for CPO + OH → products (R1) carried out 1218 K and 1.13 bar using the detailed kinetic model described in the text. The most sensitive reactions are shown in the figure legend. The OH sensitivity is defined as $S_{OH} = (\partial X_{OH} / \partial k_i) \times (k_i / X_{OH})$, where the X_{OH} is local OH mole fraction and k_i is the rate constant of the i^{th} reaction.

Table 1 compiles the overall rate coefficients for k_1 and k_2 from current measurements. Arrhenius plots of these rate coefficients are shown in Fig. 4 along with the available literature data. As stated earlier, there are no previous experimental data at high temperatures to compare

with our data. The existing theoretical studies[20-21, 28] do not accurately reproduce our experimentally measured rate coefficients, as shown in Fig. 4.

Table 1: Measured rate coefficients for the reactions of OH radical with CPO and CHO.

P_5	T_5	$k/10^{-11}$
bar	K	$cm^3molecule^{-1}s^{-1}$
Mixture 1: 400 ppm cyclopentanone, 20 ppm TBHP (~ 47 ppm water) in argon		
1.14	982	1.38
1.32	983	1.3
1.62	983	1.33
1.32	1152	1.93
1.12	1236	2.33
Mixture 2: 300 ppm cyclopentanone, 25 ppm TBHP(~ 58 ppm water) in argon		
1.26	902	1.33
1.39	924	1.38
1.58	1085	1.5
1.06	1128	1.66
1.13	1218	2.39
1.11	1222	2.44
1.41	1225	2.16
1.54	1297	2.56
Mixture 3: 300 ppm cyclohexanone, 20 ppm TBHP (~ 47 ppm water)in argon		
1.12	1023	2.16
1.27	1033	2.28
1.14	1189	3.16
Mixture 4: 300 ppm cyclohexanone, 40 ppm TBHP(~ 93 ppm water) in argon		
1.29	935	1.83
1.22	949	1.99
1.2	1107	2.66
1.11	1219	3.16
1.08	1251	3.57
1.15	1331	3.82
Mixture 5: 399.5 ppm cyclohexanone, 25 ppm TBHP(~ 60 ppm water) in argon		
1.12	890	1.74
0.90	1112	2.66

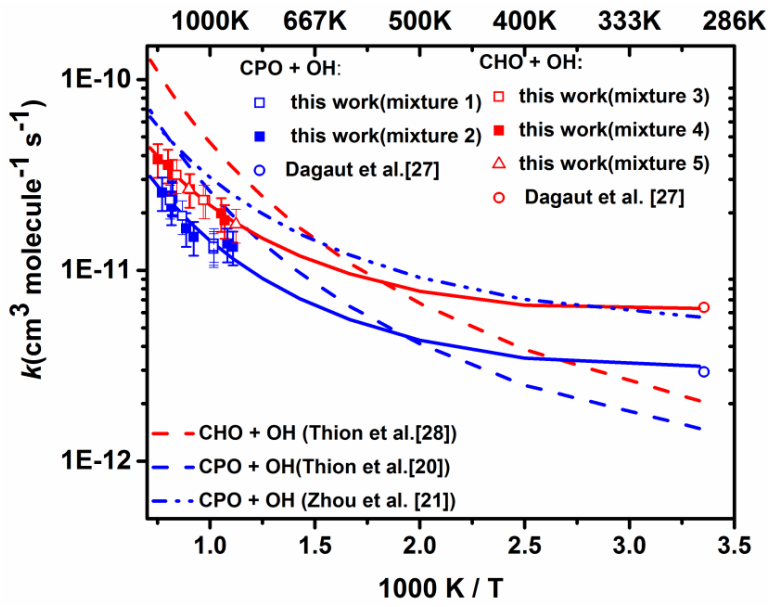

Figure 4. Arrhenius plots for the total rate coefficients of CPO + OH (R1) and CHO + OH (R2); also shown are available literature data. Solid lines represent the recommended 3-parameter Arrhenius expressions, given by Eqs. (1) and (2) of this work. Dash and dash-dot-dot lines represent literature theoretical predictions.

For CPO + OH (R1) reaction, both theoretical works[20-21] exhibit very different reactivity behavior in terms of their temperature dependence. As can be seen in Figure 4 (blue dash-dot-dot line), the predicted rate coefficients from Zhou et al.[21] run almost parallel to the experimental data while over-predicting the experimental rate coefficients by a factor of ~2. This may suggest that the calculated energy barriers for R1 are nearly accurate, but the pre-exponential factor seems to have been over-estimated. The theoretical rate coefficients from Thion et al. [20] show stronger *T*-dependance while under-predicting the single room temperature value of Dagaut et al.[27] but over-predicting our high-temperature data by roughly a factor of two. This may indicate that barrier heights predicted by Thion et al. [20] at G3//MP2/aug-cc-pVDZ level of theory are somewhat too high. At this level of theory, their predictions of all the transition states (TS) responsible for the hydrogen abstraction reactions lie higher in energy relative to the reactants (CPO + OH). On the other hand, Zhou et al.[21] predicted negative barriers for some abstraction reactions at G4 and CCSD(T)/CBS levels of theory, e.g., TS abstracting

equatorial hydrogen atoms at the α-sites (E_0 = -0.3 kcal/mol). Although the diffrence in the energy barriers is small (<1 kcal/mol) and remains within the uncertainty of the electronic energy calculations, it can have a large effect in the quality of the predicted rate coefficiens, as observed in these chemical systems.

For CHO + OH (R2) reaction, Thion et al. [28] theoretical rate coefficients over-predicated our experimental data by at least a factor of 2.5, but they under-predicted room-temperature data of Dagaut et al.[27] by a factor of 1.4. This also suggests an overestimation of the barrier heights for the abstraction pathways of R2. Therefore, the existing theoretical models need to be further tuned by anchoring with these new experimental data from this work, and update accordingly in the kinetic models. As expected, cyclohexanone (CHO) shows larger overall reactivity towards OH radicals as opposed to cyclopentanone (CPO) due to the presence of two additional hydrogen atoms at the γ-sites. Combining the high-temperature data from this work with the single room-temperature measurement from Dagaut et al.[27], the following three-parameter Arrhenius expressions are recommended for k_1 and k_2 over a wide range of temperatures:

$$k_1(\mathrm{CPO + OH}) = 1.07 \times 10^{-13} \left(\frac{T}{300\ K}\right)^{3.2} \exp\left(1005.7 \frac{K}{T}\right) \qquad 298 – 1297\ \mathrm{K} \quad \text{Eq. (1)}$$

$$k_2(\mathrm{CHO + OH}) = 3.12 \times 10^{-13} \left(\frac{T}{300\ K}\right)^{2.78} \exp\left(897.5 \frac{K}{T}\right) \qquad 298 – 1331\ \mathrm{K} \quad \text{Eq. (2)}$$

As shown in Fig. 4, Eqs. (1) and (2) reproduce the experimental data remarkably well over the entire temperature range with an average absolute deviation of 7% and 3% for k_1 and k_2, respectively. In the intermediate *T*-range, where experimental data are not yet available, Eqs. (1) and (2) are still expected to reliably estimate the rate coefficients for two reasons: i) the tunneling is not severe for these reactions, e.g., tunneling correction factors are 1.8 and 1.2 at 500 and 1000 K, respectively[21]; ii) OH addition to the carbonyl group of cyclic ketones, leading to bimolecular products, which typically shows a complex kinetic behavior, is insignificant. We

arrive to this conclusion by taking an analogy to dimethyl ketone + OH reaction where the contribution of addition channel is less than 1% over 500 – 2000 K.[36]

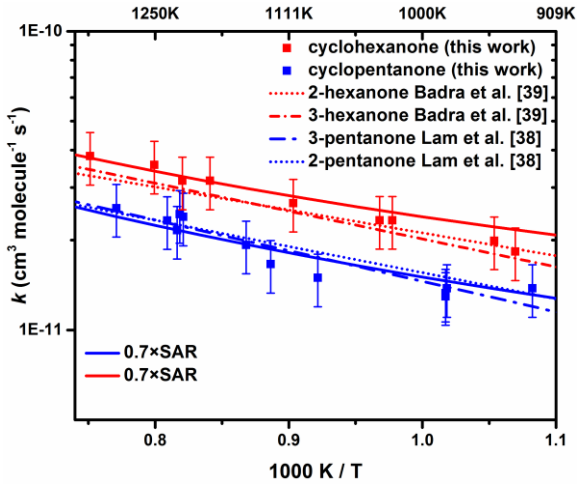

Figure 5. Comparison of the rate coefficients of cyclic ketones + OH with normal-chain ketones + OH counterparts. Also shown are predictions of structure activity relationship (SAR) multiplied by 0.7.

Figure 5 compares the reactivity of OH radicals with the cyclic ketones and their corresponding normal-chain ketone counterparts. Interestingly, within the uncertainties of the experiments, these cyclic ketones exhibit similar reactivity as their normal-chain ketone counterpart for the temperature range of 900 – 1300 K. This may just be fortuitous as we expect a little variation in the barrier heights for the hydrogen abstraction from different chemical environments of these ketones by OH radicals. For instance, the transition state for the hydrogen abstraction of CH_3-C(O)-CH_3 *via* complex formation lies about 2.4 kcal/mol above the reactant energy, whereas these are about 2.1 and 0.5 kcal/mol for CH_3-sites of CH_3-C(O)-CH_2-CH_3 adjacent to and far from the carbonyl group, respectively, and the -CH_2 site lies below the reactant by -0.1 kcal/mol. These barrier heights were calculated at G3 level of theory by Zhou et al.[36]. We caution for this sort of reaction analogy beyond 900 – 1300 K as these ketones of same carbon number do have different C-H chemical sites. As a result, they display variations in the reactivity with OH radicals as manifested by the difference in the temperature dependence

of the rate coefficients from different chemical environments. We employed the structure-activity relationship (SAR)[37] to estimate the rate coefficients for R1 and R2, and found that SAR over-estimated our experimental data. Similar reports were made by Lam et al.[38] for OH reactions with 2-butanone, 2-pentanone and 3-pentanone and by Badra et al.[39] for 2- and 3-hexanones. SAR predictions are multiplied by a factor of 0.7 to obtain a good agreement with the experimental data. We note here that similar value for the multiplicative factor (0.75) were used by earlier studies[38-39] for ketones + OH reaction systems.

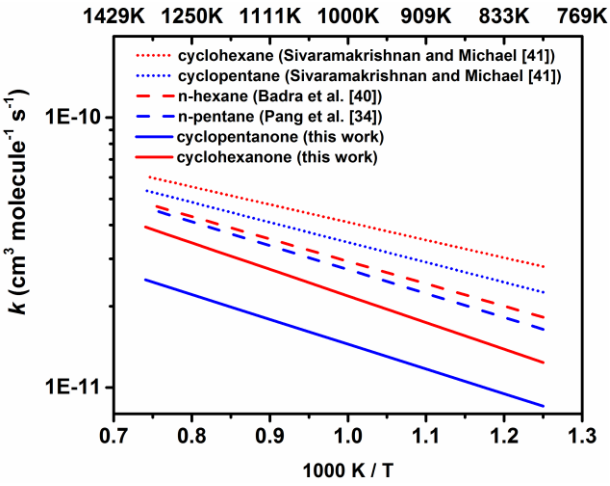

Figure 6. Reactivity trends of C_5-C_6 cyclic ketones and corresponding hydrocarbons with OH radicals.

In Fig. 6, we further compare the OH reactivity of cyclic ketones with that of C_5 – C_6 cyclic and acyclic hydrocarbons from earlier reports of Pang et al.[34], Badra et al.[40] and Sivaramakrishnan and Michael[41]. As can be seen, the reactivity trend is found to be in the order k(cyclicketone + OH) < k(alkane + OH) < k(cyclicalkanes + OH) for a given length of carbon chain. Here, a couple of things may be noted: i) not surprisingly the number of secondary abstractable hydrogen atoms matter, e.g., k(pentane + OH) < k(hexane + OH), ii) type of chemical environments also play a crucial role, e.g., k(cyclohexanone + OH) < k(cyclopentane + OH) despite of the fact that both molecules have 10 secondary hydrogen atoms, iii) total

number of abstractable hydrogen atoms matter, e.g., *k*(cyclopentanone + OH) < *k*(pentane + OH). Here, it is particularly interesting to note the slower reactivity of cyclohexanone as opposed to cyclopentane. In fact, one would expect the opposite reactivity trend since both molecules offer 10 secondary hydrogen atoms for abstraction, and the hydrogen abstraction reaction of cyclohexanone by OH radicals is expected to largely occur at α C-H sites because these are significantly weaker than β or γ C-H sites as well as the C-H sites of cyclopentane (see Fig. 7). Unexpectedly, the hydrogen abstraction reaction of OH radicals from the α-sites of cyclic ketones are found to undergo slower reaction than that of β-sites, which is in contrary to the trend observed for the hydrogen abstraction reactions of cyclic ketones by HO_2, CH_3, H and O radicals[20-21]. This observation clearly hints towards the mechanistic differences for these reactions. Generally, the hydrogen abstraction reaction of OH radicals with oxygenates undergoes *via* addition-elimination mechanism forming complexes both at the entrance and exit channels which is not the case for (a) cyclic hydrocarbons + OH reactions. Here, the reactions of cyclic ketones + OH are not the exception either in terms of complex forming reactions as shown by recent theoretical works [20-21]. These works have shown that H-abstraction at the close proximity of carbonyl group of cyclic ketones by OH radicals occurs via complex forming mechanism in an overall exothermic process, and in particular, the transition state responsible for the abstraction of α-equatorial is relatively stable due to hydrogen bonding forming a six-member ring structure. This cyclization in the transition state lowers the energy barrier and also the entropy. Here, the entropy wins the competition making β-channels react faster than α-channel. Thion et al. [20] listed the entropy changes (ΔS°) for α- and β-channel of R1, in units of cal K^{-1} mol^{-1}, to be 1.1 and 7.1 at 1000 K, respectively. This effect is not pronounced for other reactions, e.g., cyclic ketones + HO_2 [20-21], and for these reactions, the relative barrier heights largely affect their rate coefficients. As for the cyclic alkanes + OH reactions, only direct

abstraction pathways are feasible and their corresponding barrier heights display pronounced effect towards their reactivity.

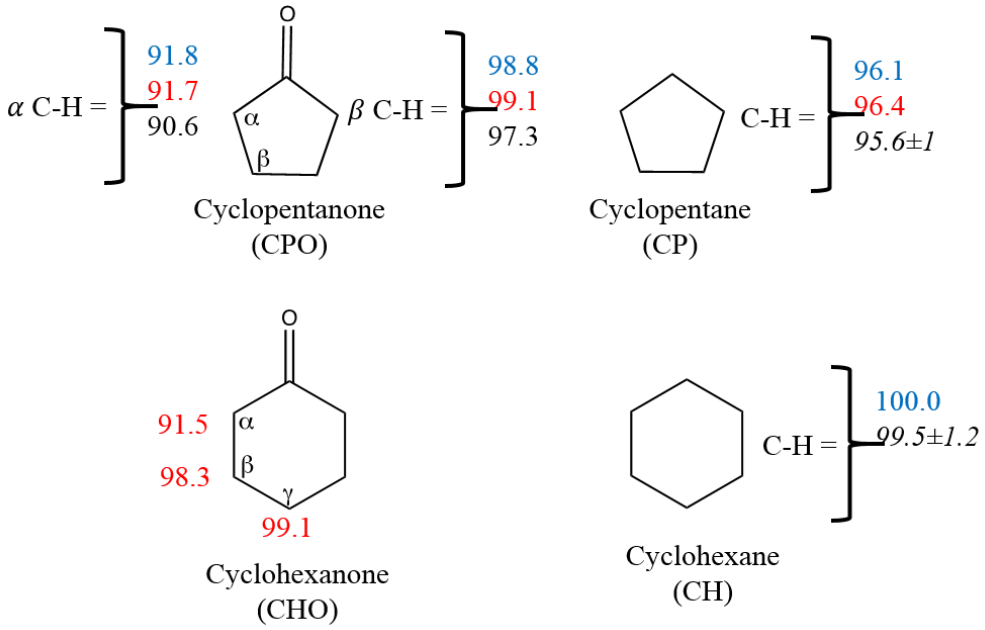

Figure 7. Comparison of the bond dissociation energies (BDEs in kcal/mol) for various C-H sites. For CPO and CP, the BDEs at CBS-QB3 (blue) and G3B3 (red) at 0 K from Thion et al.[20], G4 (black) at 298.15 K from Zhou et al.[21], experimental (italic) from Tian et al.[42]. BDEs for CHO are from Zaras et al. [24]; BDEs for cyclohexane (CH) at G3 (blue) and experimental (italic) are from Tian et al.[42].

As outlined above, the oxidation kinetics of these cyclic ketones are very sensitive to the braching ratios of reactions R1 and R2. Therefore, we make a naïve attempt to discern the site-specific rate coefficients for R1 and R2. As seen in Fig. 7, the bond dissociation energies at the α and β sites of CPO and CHO are comparable. Therefore, their reactivity towards OH at the corresponding sites can be assumed to be equal after ring strain factors are incorporated. For these reasons, we write: $k_1 = k_{1\alpha} + k_{1\beta} \approx F\,(k_\alpha + k_\beta)$ and $k_2 = k_{2\alpha} + k_{2\beta} + k_{2\gamma} \approx (k_\alpha + k_\beta + k_\gamma)$; where we use $F \sim 1$ for ring strain correction from the experimental data of Sivaramakrishnan and Michael [41]. Although Zhou et al.[21] overall theoretical rate coefficients over-predicted experimental data by roughly a factor of two, the ratio $k_\beta / k_\alpha \approx 1.65$ over 800 – 1400 K is

assumed to be valid. With $k_\beta / k_\alpha \approx 1.65$, using Eq. (1), we derive the following three parameter Arrhenius expression for k_α (in units of $cm^3 molecule^{-1} s^{-1}$):

$$k_a(T) = 4.38 \times 10^{-14} \left(\frac{T}{300\ K}\right)^{3.17} \exp\left(978.4 \frac{K}{T}\right) \qquad 800 - 1400\ K \qquad \text{Eq. (3)}$$

Thereafter, with the known values of k_α and k_β, k_γ can be deduced with the help of Eq. (2) which may be expressed by the following Arrhenius expression (in units of $cm^3 molecule^{-1} s^{-1}$):

$$k_\gamma(T) = 1.23 \times 10^{-12} \left(\frac{T}{300\ K}\right)^{1.45} \exp\left(119.5 \frac{K}{T}\right) \qquad 800 - 1400\ K \qquad \text{Eq. (4)}$$

The derived rate coefficient for k_γ agrees reasonably well, with an average deviation of +17%, with the value from Sivaramakrishnan and Michael[41] for cyclohexane + OH reaction. This slightly increased reactivity of k_γ as compared to that of cyclohexane + OH reaction may be attributed to the slightly lower (~ 1 kcal/mol) C-H bond dissociation energy (see Fig. 7).

4. Conclusions

Cyclic ketones have caught significant attention of the combustion community because they can be derived from biomass and display desirable combustion characteristics for application in future advance combustion engines. We have, for the first time, investigated hydrogen abstraction reactions of C_5-C_6 cyclic ketones by OH radicals under combustion relevant conditions. We employed shock tube/laser diagnostic technique to follow the kinetics of OH radical reactions with C_5-C_6 cyclic ketones over a wide range of temperatures (T = 900 – 1300 K). Under the current experimental conditions, cyclic ketones + OH are found to exhibit similar reactivity as that of similar carbon length acyclic ketones + OH reactions. Earlier theoretical studies are unable to accurately predict the measured rate coefficients. However, by incorporating a correction factor of 0.7, SAR captured the experimentally measured temperature dependence of the rate coefficients for R1 and R2 reasonably well. These new data

would prove beneficial to significantly improve the global performance of the oxidation kinetic models of cyclic ketones.

Associated Content

Supporting Information. The supporting information is available free of charge on the ACS Publication website at DOI:

Additional OH-times histories and simulation results using detailed kinetic models

Acknowledgements

Research reported in this publication was funded by the Office of Sponsored Research at King Abdullah University of Science and Technology (KAUST).

References

1. OECD, *Oil 2018*. OECD Publishing, Paris, 2018; p 137.
2. Kalghatgi, G. T. The Outlook for Fuels for Internal Combustion Engines. *Int. J. Engine. Res.* **2014,** *15*, 383-398.
3. Kalghatgi, G. T. Developments in Internal Combustion Engines and Implications for Combustion Science and Future Transport Fuels. *Proc. Combust. Inst.* **2015,** *35*, 101-115.
4. Kalghatgi, G. T. *Fuel/Engine Interactions*. SAE international, 2014, ISBN 978-0-7680-6458-2.

5. Sarathy, S. M.; Kukkadapu, G.; Mehl, M.; Javed, T.; Ahmed, A.; Naser, N.; Tekawade, A.; Kosiba, G.; AlAbbad, M.; Singh, E. et al. A. Compositional Effects on the Ignition of FACE Gasolines. *Combust. Flame.* **2016,** *169*, 171-193.

6. Sarathy, S. M.; Kukkadapu, G.; Mehl, M.; Wang, W.; Javed, T.; Park, S.; Oehlschlaeger, M. A.; Farooq, A.; Pitz, W. J.; Sung, C.-J. Ignition of Alkane-Rich FACE Gasoline Fuels and Their Surrogate Mixtures. *Proc. Combust. Inst.* **2015,** *35*, 249-257.

7. Farrell, J.; John Holladay, Wagner R. Fuel Blendstocks with the Potential to Optimize Future Gasoline Engine Performance: Identification of Five Chemical Families for Detailed Evaluation. Technical Report DOE/GO-102018-4970. US Department of Energy, Washington, DC, 2018.

8. Miles, P. *Efficiency Merit Function for Spark Ignition Engines: Revisions and Improvements Based on FY16–17 Research.* U.S. Department of Energy, Washington, DC, 2018.

9. Strobel, G. A.; Knighton, W.B.; Kluck, K.; Ren, Y.; Livinghouse, T.; Griffin, M.; Spakowicz, D.; Sears, J. The Production of Myco-Diesel Hydrocarbons and their Derivatives by the Endophytic Fungus Gliocladium Roseum (NRRL 50072). *Microbiology* **2010,** *156*, 3830-3833.

10. Luque, R.; Lin, C..; Wilson, K.; Clark, J. *Handbook of Biofuels Production: Processes and Technologies*. 2nd edition,Woodhead Publishing, 2016, ISBN: 9780081004555.

11. Demirbas, A. The Influence of Temperature on the Yields of Compounds Existing in Bio-Oils Obtained From Biomass Samples Via Pyrolysis. *Fuel. Process. Technol.* **2007**, *88*, 591-597.

12. Hronec, M.; Fulajtarová, K. Selective Transformation of Furfural to Cyclopentanone. *Catal. Commun*. **2012,** *24*, 100-104.

13. Engine Fuel Co-optimization Database[online]

https://fuelsdb.nrel.gov/fmi/webd/FuelEngineCoOptimization (accessed April 5, 2019).

14. Yang, Y.; Dec, J. Bio-Ketones: Autoignition Characteristics and Their Potential as Fuels for HCCI Engines. *SAE Int. J. Fuels Lubr.* **2013**, *6*, 713-728.

15. Boot, M.; Frijters, P.; Luijten, C.; Somers, B.; Baert, R.; Donkerbroek, A.; Klein-Douwel, R. J. H.; Dam, N. Cyclic Oxygenates: A New Class of Second-Generation Biofuels for Diesel Engines. *Energ. Fuel.* **2009,** *23*, 1808-1817.

16. Klein-Douwel, R. J. H.; Donkerbroek, A. J.; Vliet, A. P.; Boot, M. D.; Somers, L. M. T.; Baert, R. S. G.; Dama, N. J.; Meulen, J. J. Soot and Chemiluminescence in Diesel Combustion of Bio-derived, Oxygenated and Reference Fuels. *Proc. Combust. Inst.* **2009**, 32, 2817–2825.

17. Yang, J.; Li, N.; Li, G.; Wang, W.; Wang, A.; Wang, X.; Cong, Y.; Zhang, T. Synthesis of Renewable High-density Fuels Using Cyclopentanone Derived from Lignocellulose. *Chem. Commun. (Camb.)* **2014,** *50*, 2572-4.

18. Wang, W.; Li, N.; Li, G.; Li, S.; Wang, W.; Wang, A.; Cong, Y.; Wang, X.; Zhang, T. Synthesis of Renewable High-Density Fuel with Cyclopentanone Derived from Hemicellulose. *ACS Sustain. Chem. Eng.* **2017,** *5*, 1812-1817.

19. Zhang, K.; Lokachari. N.; Ninnemann, E.; Khanniche, S.; Green ,W. H.; Curran, H. J.; Vasu S. S.; Pitz W. J. An Experimental, Theoretical, and Modeling Study of the Ignition Behavior of Cyclopentanone. *Proc. Combust. Inst.* **2019,** *37*, 657-665.

20. Thion, S.; Togbe, C.; Dayma, G.; Serinyel, Z.; Dagaut, P. Experimental and Detailed Kinetic Modeling Study of Cyclopentanone Oxidation in a Jet-Stirred Reactor at 1 and 10 atm. *Energ. Fuel.* **2016,** *31*, 2144-2155.

21. Zhou, C. W.; Simmie, J. M.; Pitz, W. J.; Curran, H. J. Toward the Development of a Fundamentally Based Chemical Model for Cyclopentanone: High-Pressure-Limit Rate

Constants for H Atom Abstraction and Fuel Radical Decomposition. *J. Phys. Chem. A.* **2016,** *120*, 7037-7044.

22. Zaras, A. M.; Thion, S.; Dagaut, P. Computational Kinetic Study for the Unimolecular Decomposition of Cyclopentanone. *Int. J. Chem. Kinet.* **2015,** *47*, 439-446.

23. Giri, B. R., AlAbbad, M., Barker, J. R.; Farooq, A. High Temperature Unimolecular Decomposition of Cyclopentanone. *Proc. Combust. Inst.* **2018,** *37*, 267-273.

24. Zaras, A. M.; Dagaut, P.; Serinyel, Z. Computational Kinetic Study for the Unimolecular Decomposition Pathways of Cyclohexanone. *J. Phys. Chem. A.* **2015,** *119*, 7138-7144.

25. Serinyel, Z.; Togbe, C.; Zaras, A.; Dayma, G.; Dagaut, P. Kinetics of Oxidation of Cyclohexanone In a Jet-Stirred Reactor: Experimental and Modeling. *Proc. Combust. Inst.* **2015,** *35*, 507-514.

26. He, J. N.; Gou, Y.; Lu, P. F.; Zhang, C. H.; Li, P.; Li, X. Shock Tube Measurements and Kinetic Modeling Study on Autoignition Characteristics of Cyclohexanone. *Combust. Flame.* **2018,** *192*, 358-368.

27. Dagaut, P.; Wallington, T. J.; Liu, R.; Kurylo, M. J. A Kinetics Investigation of the Gas-Phase Reactions of OH Radicals with Cyclic Ketones and Diones: Mechanistic Insights. *J. Phys. Chem.* **1988,** *92*, 4375-4377.

28. Thion, S.; Serinyel, Z.; Dayma, G.; Dagaut, P. More Insight Into Cyclohexanone Oxidation: Jet-stirred Reactor Experiments and Kinetic Modeling. *Fuel* **2018,** *220*, 908-915.

29. Badra, J.; Khaled, F.; Giri, B. R.; Farooq, A. A Shock Tube Study of the Branching Ratios of Propene + OH Reaction. *Phys. Chem. Chem. Phys.* **2014,** *17*, 2421-2431.

30. Khaled, F.; Giri, B. R.; Farooq, A. A High-Temperature Shock Tube Kinetic Study for the Branching Ratios of Isobutene + OH Reaction. *Proc. Combust. Inst.* **2017,** *36*, 265-272.

31. Bradley, J., *Shock waves in physics and chemistry*. Methuen, London **1962**.

32. Campbell, M. F.; Haylett, D. R.; Davidson, D. F.; Hanson, R. K. AEROFROSH: A Shock Condition Calculator for Multi-Component Fuel Aerosol-Laden Flows. *Shock Waves* **2016**, 26, 429-447.

33. Vasudevan, V.; Davidson, D. F.; Hanson, R. K. High-temperature Measurements of the Reactions of OH with Toluene and Acetone. *J. Phys. Chem. A.* **2005,** *109*, 3352-3359.

34. Pang, G. A.; Hanson, R. K.; Golden, D. M.; Bowman, C. T. High-Temperature Measurements of the Rate Constants for Reactions of OH with a Series of Large Normal Alkanes: n-Pentane, n-Heptane, and n-Nonane. *Z. Phys. Chem.* **2011,** *225*, 1157-1178.

35. CHEMKIN-PRO, Reaction Design: San Diego, 2015.

36. Zhou, C.W.; Simmie, J. M.; Curran, H. J. Ab Initio and Kinetic Study of the Reaction of Ketones with OH for T = 500-2000 K. Part I: hydrogen-abstraction from $H_3CC(O)CH_{(3-x)}(CH_3)_x$, x = 0 - 2. *Phys. Chem. Chem. Phys.* **2011,** *13*, 11175-11192.

37. Kwok, E. S. C.; Atkinson, R. Estimation of Hydroxyl Radical Reaction Rate Constants for Gas-phase Organic Compounds Using a Structure-Reactivity Relationship: An Update. *Atmos. Environ.* **1995,** *29*, 1685-1695.

38. Lam, K. Y.; Davidson, D. F.; Hanson, R. K. High-temperature Measurements of the Reactions of OH with a Series of Ketones: Acetone, 2-butanone, 3-pentanone, and 2-pentanone. *J. Phys. Chem. A.* **2012,** *116*, 5549-5559.

39. Badra, J.; Elwardany, A. E.; Farooq, A. Reaction Rate Constants of H-abstraction by OH from Large Ketones: Measurements and Site-specific Rate Rules. *Phys. Chem. Chem. Phys.* **2014,** *16*, 12183-12193.

40. Badra, J.; Elwardany, A.; Farooq, A. Shock Tube Measurements of the Rate Constants for Seven Large Alkanes Plus OH. *Proc. Combust. Inst.* **2015,** *35*, 189-196.

41. Sivaramakrishnan, R.; Michael, J. V. Shock Tube Measurements of High Temperature Rate Constants for OH with Cycloalkanes and Methylcycloalkanes. *Combust. Flame.* **2009,** *156*, 1126-1134.

42. Tian, Z.; Fattahi, A.; Lis, L.; Kass, S. R. Cycloalkane and Cycloalkene C−H Bond Dissociation Energies. *J. Am. Chem. Soc.* **2006,** *128*, 17087-17092.

TOC Graphic:

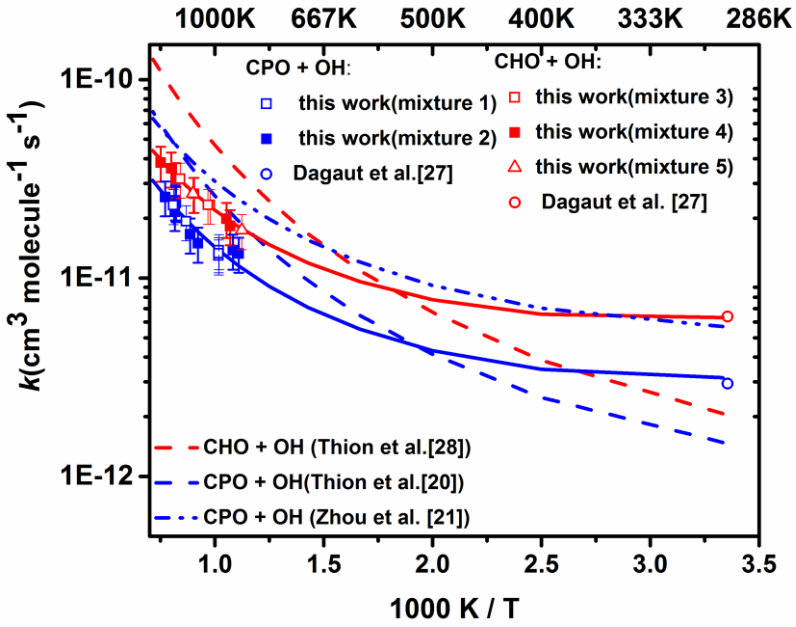
1000K
667K
500K
400K
333K
286K
CPO + OH:
this work(mixture 1)
this work(mixture 2)
Dagaut et al.[27]
CHO + OH:
this work(mixture 3)
this work(mixture 4)
this work(mixture 5)
Dagaut et al. [27]
CHO + OH (Thion et al.[28])
CPO + OH(Thion et al.[20])
CPO + OH (Zhou et al. [21])
1E-10
1E-11
1E-12
k(cm3 molecule-1 s-1)
1.0
1.5
2.0
2.5
3.0
3.5
1000 K / T